

Pauli Check Extrapolation for Quantum Error Mitigation

Quinn Langfitt^{1,*}, Ji Liu^{1,*}, Benchen Huang², Alvin Gonzales¹,

Kaitlin N. Smith³, Nikos Hardavellas³, and Zain H. Saleem¹

¹*Mathematics and Computer Science Division, Argonne National Laboratory, Lemont, IL, USA*

²*Department of Chemistry, University of Chicago, Chicago, IL, USA and*

³*Department of Computer Science, Northwestern University, Evanston, IL, USA*

Pauli Check Sandwiching (PCS) is an error mitigation scheme that uses pairs of parity checks to detect errors in the payload circuit. While increasing the number of check pairs improves error detection, it also introduces additional noise to the circuit and exponentially increases the required sampling size. To address these limitations, we propose a novel error mitigation scheme, Pauli Check Extrapolation (PCE), which integrates PCS with an extrapolation technique similar to Zero-Noise Extrapolation (ZNE). However, instead of extrapolating to the ‘zero-noise’ limit, as is done in ZNE, PCE extrapolates to the ‘maximum check’ limit—the number of check pairs theoretically required to achieve unit fidelity. In this study, we focus on applying a linear model for extrapolation and also derive a more general exponential ansatz based on the Markovian error model. We demonstrate the effectiveness of PCE by using it to mitigate errors in the shadow estimation protocol, particularly for states prepared by the variational quantum eigensolver (VQE). Our results show that this method can achieve higher fidelities than the state-of-the-art Robust Shadow (RS) estimation scheme, while significantly reducing the number of required samples by eliminating the need for a calibration procedure. We validate these findings on both fully-connected topologies and simulated IBM hardware backends.

I. INTRODUCTION

Quantum error mitigation is essential for the practical application of noisy intermediate-scale quantum (NISQ) devices in various fields, including machine learning [1], combinatorial optimization [2], quantum simulation [3], and cryptography [4]. Several error mitigation techniques have been developed to improve the performance of NISQ devices, such as zero-noise extrapolation (ZNE) [5–7], probabilistic error cancellation [8], Pauli Check Sandwiching (PCS) [9, 10], symmetry verification [11–14], and simulated quantum error mitigation [15].

Zero-Noise Extrapolation (ZNE) is an error mitigation technique that reduces noise in quantum circuits by artificially amplifying the noise intensity in the circuit. This can be achieved by inserting logical identity operations into the circuit which increase the noise without altering the intended computations. ZNE then measures the expectation values of the circuit at varying noise intensities and uses these measurements to extrapolate back to a zero-noise limit. By applying a regression model to these data points, ZNE predicts the output of the circuit as if it were operating in an ideal, noise-free environment.

Pauli Check Sandwiching (PCS) mitigates errors in the computational circuit by imposing constraints on the circuit and post-selecting on the outputs that violate those constraints. Pauli gates are applied at both ends of the circuit with an ancilla qubit appended for each pair of checks. Since the checks are applied in a layering fashion on the original circuit, each pair of checks is typically referred to as a ‘layer.’ Each sample is then followed by a

measurement of the ancilla qubit(s), where only the results corresponding to zero(s) on the ancilla(s) are kept, therefore acting as a post-selection scheme. In the limit that the checks are ideal, Proposition 2 in [10] states that there exist $2n$ number of PCS checks (possibly employing checks not in the Pauli group), where n is the number of compute qubits, such that the postselected state is noiseless. The checks consist of left and right pairs and we can always employ weight-one Pauli checks for one of the checks for each pair.

In this work, we introduce Pauli Check Extrapolation (PCE), which integrates an extrapolation technique with PCS to extend our expectation value calculations to the ‘maximal check’ limit. Employing an approach similar to ZNE, we develop a model—linear or exponential—and fit it to the data points corresponding to the expectation values for each check using least squares fitting. We then extrapolate the expectation value to the maximum limit of checks. Like ZNE, this simulates the effect of adding additional layers of checks to estimate the expectation value at the maximum check limit. PCS allows us to reduce noise, whereas traditional ZNE requires the increase in noise levels, which may not be suitable for highly noisy circuits. Additionally, extrapolation methods are typically more accurate when the collected data points are near the target domain value. Thus, a very important advantage of our scheme over ZNE is that we do not need to sample circuits with a significantly larger gate count than the original circuit we are mitigating. Our approach also avoids the noise typically associated with the physical implementation of additional check layers and eliminates the exponentially increasing sampling overhead with each added layer. Additionally, for non-Clifford circuits where the number of applicable Pauli checks is limited, we can extrapolate to checks that can-

* These authors contributed equally.

not be physically performed, thus bypassing this limitation.

We apply PCE to improve the accuracy of the shadow estimation scheme for the variational quantum eigensolver (VQE) [16]. We compare our results with that of the state-of-the-art Robust Shadow (RS) estimation scheme [17]. Our simulations employ circuits with depolarizing noise affecting each single-qubit and two-qubit gate, including the checks. Under fully-connected qubit topologies, we find that the extrapolated PCS technique significantly improves fidelity over the RS estimation for a 4-qubit H_2 VQE circuit when the entire circuit (including state preparation and shadow portions) is protected. We also demonstrate comparable or even improved fidelities for the 6-qubit H_2O VQE circuit under homogeneous and inhomogeneous noise distributions, respectively. Furthermore, we find that PCE technique can offer comparable, and sometimes improved, performance on fake IBM hardware backends, depending on the device connectivity.

In addition to improved performance, we note that the PCE technique does not require a calibration procedure, unlike RS estimation. By eliminating this calibration step, PCE offers the additional benefit of reducing the total required sampling size. This advantage is significant, even if the fidelity is slightly lower for some instances.

II. BACKGROUND

A. Pauli Check Sandwiching

PCS sandwiches the target computational circuit, denoted by U , between pairs of controlled Pauli gates. Mathematically, these Pauli gates are chosen from the Pauli group $\mathcal{P}_n = \{I, X, Y, Z\}^{\otimes n} \times \{\pm 1, \pm i\}$. The controlled Pauli gates, $L, R \in \mathcal{P}_n$, are selected such that

$$LUR = U. \quad (1)$$

To detect errors, an ancilla qubit is appended to the system for each layer of Pauli checks. The detection of an error is indicated by a measurement outcome of 1 on the ancilla qubit(s). Conversely, a measurement outcome of 0 on all ancilla qubits signifies no detected errors, and thus, the results of the computation are kept. Through this process of post-selection, PCS effectively mitigates the impact of errors in the computational circuit. An example of a circuit with one layer of Pauli checks is shown in Fig. 1.

We can introduce additional layers to our circuit, where each pair of Pauli gates L_n, R_n , where n is the layer number, satisfy the condition in Eq. 1. This will theoretically allow the circuit to detect more errors and therefore improve the state fidelity. Furthermore, as stated in Proposition 2 of [10], in the theoretical limit of noiseless checks, there exists a set of checks (which

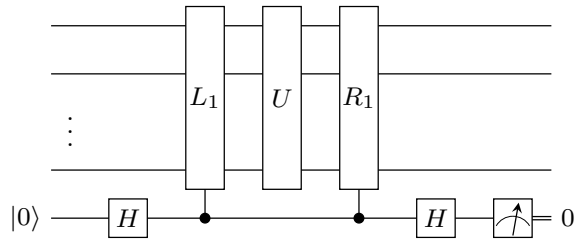


FIG. 1: Pauli Check Sandwiching circuit with a single layer of checks. Here U is the compute circuit.

may include non-Pauli checks for general circuits) that ensures the post-selected state is noiseless. An example of a circuit with multiple layers is shown in Fig. 2.

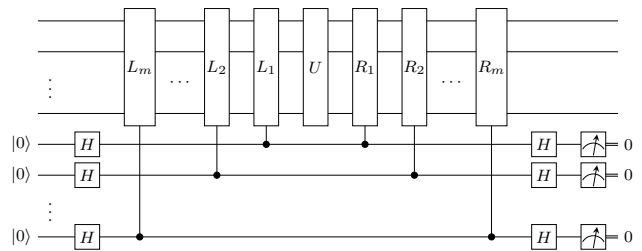


FIG. 2: Pauli Check Sandwiching circuit with multiple layers. Here U is the compute circuit.

B. Classical Shadow Tomography

The goal of shadow tomography [18] is to predict the expectation value of M physical observables for a certain quantum state (simultaneously) from relatively few measurements. It works by i). performing random measurements over the quantum state and ii). estimating all the expectation values through post-processing measurement outcomes. Shadow tomography is an approximate theory, and it requires a number of samples:

$$N = O\left(\log(M) \max_i \|O_i\|_{\text{shadow}}^2 / \epsilon^2\right),$$

to keep errors for the estimation of each observable within ϵ . What's essential about this protocol is that the number of samples required only scales logarithmically with M , making it promising for practical quantum simulation applications [19–21]. In the above equation, $\|O_i\|_{\text{shadow}}$ denotes the shadow norm of the i -th observable, which depends on the set of randomized measurements we use. For our experiments, we use the global Clifford group $\text{Cl}(2^n)$, which has a shadow norm of $\|O_i\|_{\text{shadow}} < 3 \text{tr}(O^2)$.

To apply PCS to classical shadow tomography, we can sandwich the global Clifford at the end of the circuit. For any given Pauli check P_2 , there will always exist

a corresponding Pauli check P_1 for a circuit with only Clifford gates. This configuration is theoretically guaranteed to protect that portion of the circuit up to unit fidelity if the checks are noiseless (Theorem 1 in [10]). Alternatively, we can include both the state preparation circuit and the random global Clifford. An advantage of extrapolation is that, when including the state preparation circuit—potentially a non-Clifford circuit—we can extrapolate to checks that cannot be physically applied. This is important because the number of pairs L and R that satisfy Eq. 1 decreases with the number of non-Clifford gates. Moreover, for larger quantum circuits, we can theoretically guarantee finding pairs of Pauli checks for portions of the circuit by focusing on protecting blocks of Clifford circuits. We present results for both configurations in Section IV.

C. Robust Shadow Estimation

RS estimation [17, 22] is a protocol designed for mitigating errors in the shadow circuit, originally for global/local Clifford group $\text{Cl}(2^n), \text{Cl}_2^{\otimes n}$, and recently generalized to the fermionic case [23, 24]. This protocol could in principle recover the noise-free expectation value if i). the state preparation is perfect, and ii). the shadow circuit noise is gate-independent, time-stationary, and Markovian (GTM).

The scheme operates by first characterizing the noisy channel of classical shadow estimation, which is ultimately used to compensate for the effect of noise during post-processing. This characterization is accomplished through a calibration procedure involving sampling over shadow circuits. This calibration contributes to a significant sampling overhead compared to PCS, which does not require such a step. Theorem 7 in Ref. [17] states that when sampling from the global Clifford group, the number of total required samples is

$$R = 136 \ln(2\delta^{-1}) \frac{(1 + \varepsilon^2)(1 + \frac{1}{d})^2}{\varepsilon^2(F_Z - \frac{1}{d})^2},$$

where ε sets the threshold for calibrating the noise channel with a success probability of at least $1 - \delta$, d represents the dimension of the problem, and F_Z is called the Z -basis fidelity of the noise channel which can be approximated as unity when the noise is small [17]. Although we note that the sampling complexity is (approximately) independent of system size when the noise is small, in practice this calibration step can introduce a fairly large sampling overhead. For example, if we set $\varepsilon = 1\%$, this increases the number of samples by a factor of $1/\varepsilon^2 = 10,000$ to the already existing 136 pre-factor. These additional calibration samples can be challenging to implement on real hardware.

III. METHODOLOGY

A. Pauli Check Extrapolation

The PCS scheme faces the following challenges:

1. On real hardware, each additional layer of checks introduces more noise into the circuit.
2. The post-selection rate decreases exponentially with the increase in the number of layers.
3. For non-Clifford circuits, the number of Pauli checks we can apply is limited.

To overcome these limitations, we propose an extrapolation technique that simulates the effect of maximizing the number of PCS layers without physically implementing them. This maximum layer count is tailored to the system size and the specific observables required; for instance, only incorporating a controlled Pauli Z gate for each qubit when measurements are solely in the Z -basis. Extrapolation effectively bypasses the additional noise and sampling overhead that would result from actually implementing additional layers. Additionally, for non-Clifford circuits where the number of applicable Pauli checks is limited, extrapolation allows us to bypass this limitation, provided we can at least find a few checks.

The extrapolation can be done as follows: First, we implement the first m layers of Pauli checks on the quantum circuit and measure the corresponding expectation values $E_{i_{n=1}}^m$. The collected expectation values form a dataset (n, E_n) , where n represents the number of check layers and E_n is its corresponding measured expectation value.

Next, we assume an extrapolation model $E(n)$ to fit the collected data. For example, the model could be a linear model with the form $E(n) = \alpha + \beta n$, where n is the number of check layers, and α and β are the regression coefficients. We apply linear regression to the dataset (n, E_n) to determine the optimal parameters α and β by minimizing the sum of squared differences between the observed expectation values E_n and the predicted values $\alpha + \beta n$. Different choices of the extrapolation model can produce different results, and while we primarily use a linear model, other models such as polynomial or exponential can also be considered. For instance, an exponential model can be expressed as $E(m) = ab^m + c$, where a , b , and c are fitting parameters.

Once the model is fitted, we use it to extrapolate the expectation value to the theoretical maximum number of check layers n_{\max} . The extrapolated expectation value $E(n_{\max}) = \alpha + \beta n_{\max}$ provides an estimate as if the circuit had n_{\max} check layers that would theoretically achieving unit fidelity. Figure 3 visually depicts the extrapolation process.

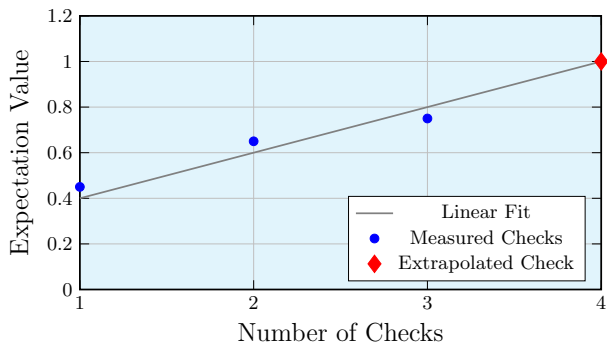


FIG. 3: Schematic of a linear model fitted to the expectation values for each physically implemented check layer (blue circle) and extrapolating to the fourth check (red diamond).

B. Expectation Value Ansatz

We can use the Markovian error model described in Ref. [25] to derive an ansatz for the expectation value. Let π_1 , π_2 , and π_3 denote the states of detected error, undetected error, and no error, respectively. Let ϵ denote the probability of an error on the data qubits. Initially (without checks), the state of the quantum computer is described by the vector

$$\vec{\pi} = \begin{pmatrix} \pi_1^{(0)} \\ \pi_2^{(0)} \\ \pi_3^{(0)} \end{pmatrix} = \begin{pmatrix} 0 \\ \epsilon \\ 1 - \epsilon \end{pmatrix} \quad (2)$$

and the transition matrix for each check is given by the upper triangular matrix

$$T = \begin{pmatrix} 1 & \frac{1}{2} & t_d \\ 0 & \frac{1}{2} & t_u \\ 0 & 0 & t_{ok} \end{pmatrix}, \quad (3)$$

where t_d , t_u , t_{ok} are the probabilities of the check introducing a detectable error, an undetectable error, and no error, respectively [25]. The probability of a logical error is given by

$$P(\text{logical error}) = \frac{\pi_2}{\pi_2 + \pi_3}. \quad (4)$$

Since we are interested in the logical error, we can ignore the detected error state and focus on the block matrix

$$T' = \begin{pmatrix} \frac{1}{2} & t_u \\ 0 & t_{ok} \end{pmatrix}. \quad (5)$$

Let the checks be near perfect, i.e., $t_d = 0$, $t_u = 0$, and $t_{ok} = 1$. The logical error rate after m checks for this scenario is

$$P(\text{logical error}) = \frac{\left(\frac{1}{2}\right)^m \epsilon}{1 - \epsilon + \left(\frac{1}{2}\right)^m \epsilon} = \frac{\epsilon}{2^m(1 - \epsilon) + \epsilon}, \quad (6)$$

which is exponential in m . Therefore, the expectation value as a function of the number of checks m should also be exponential. In this paper, we use the form

$$E(m) = ab^m + c, \quad (7)$$

where a , b , and c are scalars determined from fitting. This result is intuitive because the set of undetectable commuting Pauli strings exponentially decreases (by a factor of $\frac{1}{2}$) with each check.

IV. RESULTS

A. Experimental Setup

In the following set of experiments, we focus on the application of error mitigating the expectation value of tensor products of Pauli operators derived from classical shadow tomography for VQE circuits. We focus on two examples: a 4-qubit circuit for modeling the H_2 molecule and a 6-qubit circuit for H_2O . The circuit for the H_2 molecule is shown in Fig. 4. For classical shadow tomography, a random global Clifford circuit unitary is appended to the VQE circuit, followed by Z -basis measurements.

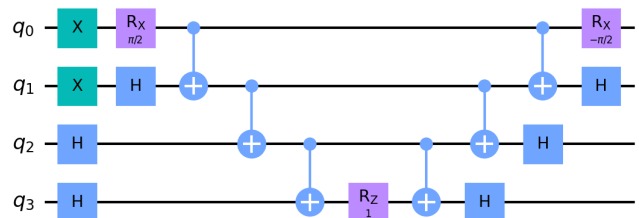


FIG. 4: State preparation circuit for the H_2 molecule using 4 qubits. The variational parameters in the circuit is optimized from a prior noiseless VQE calculation.

A widely used type of ansatz for solving the eigenvalue problem of molecular and solid-state systems is the unitary coupled-cluster (UCC) [26] circuit, which is inspired from coupled-cluster theory [27]. UCC ansatz is systematically improvable but suffers from long circuit depth, which makes it hard for near-term quantum hardware. A workaround is the qubit coupled-cluster (QCC) [28] ansatz, which reduces the circuit depth significantly by a pre-screening procedure. For the circuits used in this work, we adopted the QCC circuits with variational parameters optimized from a prior noiseless VQE calculation.

In our experiments, we compare four types of scenarios when executing our VQE circuits with classical shadow tomography: the ideal noiseless circuit, the noisy circuit without any error mitigation, the noisy circuit with robust shadow estimation applied, and the noisy circuit with various number of check layers implemented.

For a given state preparation circuit, we generate 10000 shadow circuits by appending random global Cliffords to the VQE circuit. We then collect a total of 100 computational basis measurement samples from each circuit. We post-process the measurement data by estimating observables across various number of shadow circuits N , which include 100, 400, 1000, 4000, and 10000 shadow circuits. For each shadow circuit number, we sample N shadow circuits from the total pool. These N shadow circuits are then partitioned into 20 equally sized sets, each containing $N/20$ circuits. To reduce the effect of outliers, we compute the mean observable estimate for each set and then take the median of these means for each number of shadow circuits. This process follows the procedure outlined in Algorithm 1 from [18].

In this implementation of PCS within classical shadow tomography, the measurement is conducted exclusively in the Z -basis. Therefore, errors on the phase do not impact the output, limiting the utility of checks beyond the number of qubits in the compute circuit. Accordingly, we use the first 3 check expectation values to extrapolate to a maximum of 4 checks for the H_2 circuit and use the first 4 checks to extrapolate to 6 checks for the H_2O circuit.

B. Fully connected topology

We begin by examining a fully connected topology where each gate, including single-qubit and two-qubit gates, is subjected to depolarizing noise. The error rates are denoted as p_1 for single-qubit gates and p_2 for two-qubit gates. We allow the depolarizing noise to affect all gates in the circuit, including the checks L_n and R_n .

As mentioned in Section II, in the context of a Clifford circuit, it is always possible to identify a Pauli check L_n corresponding to any given R_n such that the condition in Eq. 1 is satisfied. Figure 5 illustrates the scenario where the global Clifford at the end of the circuit in the classical shadow protocol is protected, denoted as ‘check4’ and ‘check4 (extrap)’. A distinct advantage of PCS over robust shadow estimation is its capability to extend protection to the state preparation portion of the circuit, in addition to the global Clifford. This extended protection is evident in Figure 5, where PCS outperforms robust shadow estimation by error mitigating the entire circuit. We can also see in Figure 5 that the extrapolated check provides similar performance to its actual check implementation, suggesting that the extrapolation technique accurately predicts the associated expectation values for the maximal check layer implementation. We noticed similar accuracy across all the scenarios we tested, including the IBM fake backends we test in Section IV C.

Extending our analysis to the 6-qubit H_2O circuit, we find that PCS, when extrapolated to the maximum of six layers, performs comparably to robust shadow estimation as we scale up the circuit size. This observation is supported by the results shown in Figure 6. Moreover,

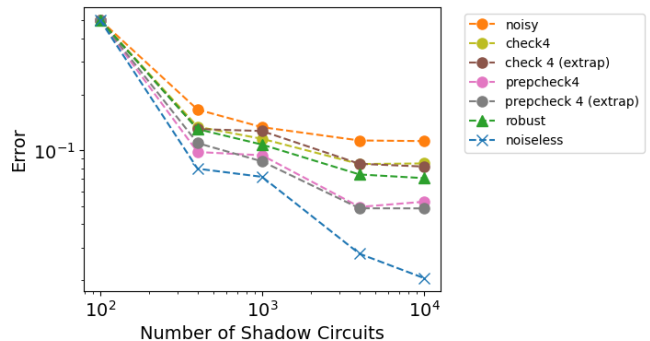


FIG. 5: 4-qubit H_2 circuit with full connectivity under a depolarizing error channel ($p_1 = 0.002$, $p_2 = 0.02$).

Results compare protecting only the Clifford portion (Check) versus the entire circuit (PrepCheck). ‘Check 4 (extrap)’ and ‘PrepCheck 4 (extrap)’ show extrapolated expectation values from the first three check implementations.

RS estimation generally assumes a uniform noise distribution, (assumption **A1** in [17]), which is often not the case in real hardware where error rates can vary between qubits, even for the same quantum gate [29]. However, PCS does not make any such assumptions on the error model of the circuit.

Figure 6b shows the results when we apply a random Gaussian distribution of error rates across the qubits, with mean error rates of $p_2 = 0.02$ and $p_1 = 0.002$ and standard deviations of 0.005 and 0.0005, respectively. The advantage of PCS over RS in mitigating circuits with inhomogeneous noise distribution is evident, as PCS shows lower error rates in the presence of unevenly distributed noise for extrapolated check 6 compared to robust shadow estimation. This improvement suggests that PCS may perform better under more realistic error rates that reflect real-world quantum computing environments.

C. IBM device topology

In this subsection, we analyze PCS performance using realistic noise models and circuit topologies that mimic IBM quantum devices, specifically using mock backends provided by Qiskit. Here we focus on only the case where PCS protects the entire 4-qubit H_2 shadow circuit (both state preparation and Clifford portions) and compare the results to RS.

Figure 7 shows the performance of PCS on two IBM mock backends: Cairo and Melbourne. We allow the error rates provided by the backends to affect the entire circuit, including the controlled Pauli checks. By protecting both the state preparation and the Clifford portions of the circuit, PCS, when extrapolated to four layers, shows performance comparable to that of robust shadow estimation. Additionally, the error rate curves across the number of check layers follow a similar trend, even when

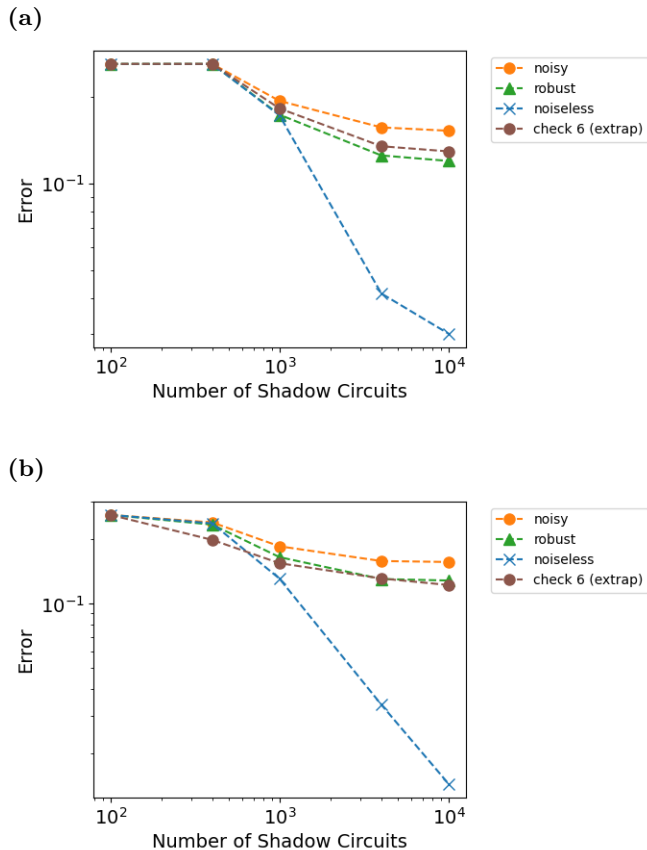


FIG. 6: Fully connected 6-qubit H_2O circuit under different error conditions. (a) has a homogeneous depolarising error rate across all qubits of $p_1 = 0.002$ and $p_2 = 0.02$ while (b) has varying depolarizing error with two-qubit error rate $p_2 = 0.02 \pm 0.005$, and mean single-qubit error rate $p_1 = 0.002 \pm 0.0005$.

extrapolating the final fourth check. This trend suggests that the extrapolation model is well suited even for noise models which are not exclusively depolarizing.

We have also tested various other IBM mock backends and observed a similar trend: PCS can perform comparably to RS estimation, and in some cases, offer slightly improved fidelities, but this improvement was only evident when the entire circuit was protected. Our analysis suggests that the performance of PCS depends more on the topology of the circuit than on the specific types of noise. This difference in performance is noticeable when comparing the results from Figure 5 to Figure 7. In Figure 5, the difference between PCS PrepCheck4 and RS is significantly greater than in Figure 7, where PCS PrepCheck4 and RS perform almost equally.

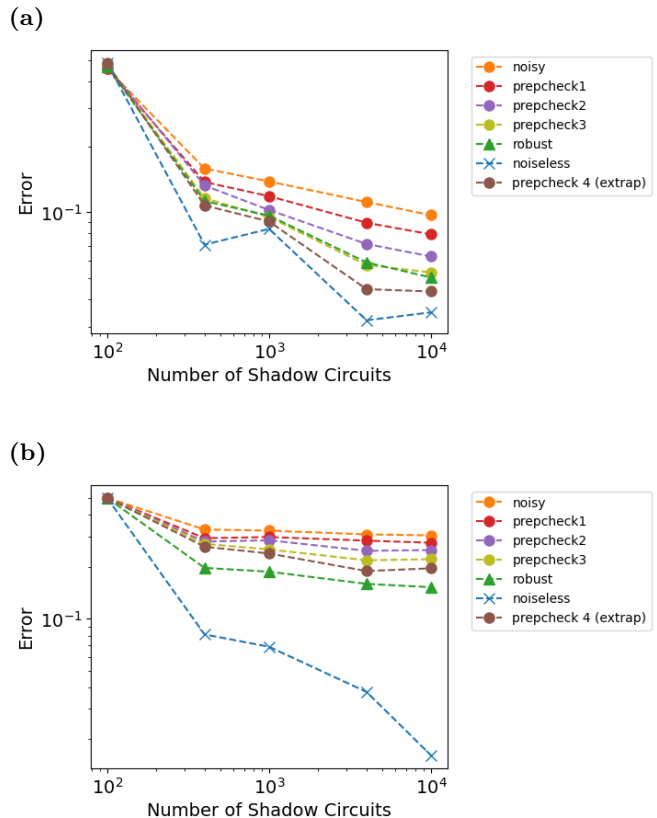


FIG. 7: 4-qubit H_2 circuit with realistic device connectivity and noise models. Both panels demonstrate the protection of the state preparation and Clifford portions of the circuit, referred to as ‘PrepCheck’: (a) Cairo device and (b) Melbourne device.

V. CONCLUSIONS AND FUTURE DIRECTIONS

In this paper, we introduced a novel error mitigation scheme that extends upon PCS by extrapolating the checks from the physically implemented checks. This approach helps us to achieve similar fidelities associated with the maximum number of checks while avoiding the practical issues such as the additional noise and the exponentially decreasing postselection rate that arise from physically adding more checks. We applied our scheme to mitigate errors in the classical shadow scheme and demonstrated that it can offer equal or superior performance compared to the current state-of-the-art classical shadow error mitigation scheme. Additionally, a key advantage of our scheme over the RS method is that it does not require a calibration step, which significantly reduces the overall number of samples needed for implementation.

One future direction is to evaluate how PCE performs when protecting the Clifford portion and a partial amount of the state preparation circuit. This ap-

proach is particularly relevant when the number of non-Clifford gates is significantly large, as is often the case with increasing system sizes in VQE circuits, making it impractical to find Pauli checks to protect the entire state preparation circuit. Our results show that optimal performance is achieved when the entire circuit, rather than just the Clifford circuit, is sandwiched. Protecting both the state preparation and Clifford circuits is another advantage of the PCS scheme over RS estimation. However, a key consideration is the trade-off between performance and the time required to search for Pauli checks when including non-Clifford portions of the circuit.

Additionally, extending PCE to larger quantum circuits is another important future direction. As system sizes grow and circuits become more complex, particularly those with a higher number of non-Clifford gates, it becomes increasingly important to evaluate the scalability of PCE. This includes investigating the efficiency and practicality of finding suitable Pauli checks for large-scale circuits and exploring the performance trade-offs involved.

For this paper, we utilized a linear ansatz to extrapolate expectation values from our check implementations. Additionally, we tested a more general exponential ansatz, $E(m) = a(b)^m + c$, where a , b , and c are scalars determined through fitting. This model was derived in Section IIIB using the Markovian model described in Ref. [25]. In our tests, the exponential model produced

results similar to the linear model, with the fitted parameter b often being very close to 1, effectively resulting in a linear fit. It is possible that the exponential model may perform better with a larger number of checks or under different noise models. Additionally, other models used in ZNE, such as various polynomial ansatzes, could be tested to improve performance.

Finally, another future direction is to test PCE on real quantum devices with fully connected architectures. The effectiveness of PCE appears to be significantly influenced by the device’s connectivity, likely due to the additional noise overhead introduced by the checks themselves, as the noise overhead imposed on the compute circuit U would likely be detected by the Pauli checks and thus mitigated. Testing on fully or near-fully connected hardware will provide further insights into the practical performance and robustness of PCE in mitigating errors in real-world quantum computing environments.

VI. ACKNOWLEDGEMENTS

QL, JL, BH, ZHS, and AG acknowledge support by the Q-NEXT Center. NH and KNS acknowledge support from NSF award CCF-2119069 and Northwestern University’s McCormick School of Engineering.

-
- [1] I. S. Maria Schuld and F. Petruccione, *Contemporary Physics* **56**, 172 (2015), <https://doi.org/10.1080/00107514.2014.964942>.
 - [2] E. Farhi, J. Goldstone, and S. Gutmann, “A quantum approximate optimization algorithm,” (2014), arXiv:1411.4028 [quant-ph].
 - [3] Y. Li and S. C. Benjamin, *Phys. Rev. X* **7**, 021050 (2017).
 - [4] H. Buhrman, N. Chandran, S. Fehr, R. Gelles, V. Goyal, R. Ostrovsky, and C. Schaffner, *SIAM Journal on Computing* **43**, 150–178 (2014).
 - [5] K. Temme, S. Bravyi, and J. M. Gambetta, *Phys. Rev. Lett.* **119**, 180509 (2017).
 - [6] Y. Kim, C. J. Wood, T. J. Yoder, S. T. Merkel, J. M. Gambetta, K. Temme, and A. Kandala, *Nature Physics* **19**, 752–759 (2023).
 - [7] A. Kandala, K. Temme, A. D. Córcoles, A. Mezzacapo, J. M. Chow, and J. M. Gambetta, *Nature* **567**, 491–495 (2019).
 - [8] S. Endo, S. C. Benjamin, and Y. Li, *Physical Review X* **8** (2018), 10.1103/physrevx.8.031027.
 - [9] D. M. Debroy and K. R. Brown, *Phys. Rev. A* **102**, 052409 (2020).
 - [10] A. Gonzales, R. Shaydulin, Z. H. Saleem, and M. Suchara, *Scientific Reports* **13** (2023), 10.1038/s41598-023-28109-x.
 - [11] X. Bonet-Monroig, R. Sagastizabal, M. Singh, and T. E. O’Brien, *Physical Review A* **98** (2018), 10.1103/physreva.98.062339.
 - [12] S. McArdle, X. Yuan, and S. Benjamin, *Physical Review Letters* **122** (2019), 10.1103/physrevlett.122.180501.
 - [13] R. Shaydulin and A. Galda, in *2021 IEEE International Conference on Quantum Computing and Engineering (QCE)* (IEEE, 2021).
 - [14] Z. Cai, *Quantum* **5**, 548 (2021).
 - [15] J. Liu, A. Gonzales, and Z. H. Saleem, “Classical simulators as quantum error mitigators via circuit cutting,” (2022), arXiv:2212.07335 [quant-ph].
 - [16] A. Peruzzo, J. McClean, P. Shadbolt, M.-H. Yung, X.-Q. Zhou, P. J. Love, A. Aspuru-Guzik, and J. L. O’Brien, *Nature Communications* **5**, 4213 (2014).
 - [17] S. Chen, W. Yu, P. Zeng, and S. T. Flammia, *PRX Quantum* **2** (2021), 10.1103/prxquantum.2.030348.
 - [18] H.-Y. Huang, R. Kueng, and J. Preskill, *Nature Physics* **16**, 1050–1057 (2020).
 - [19] W. J. Huggins, B. A. O’Gorman, N. C. Rubin, D. R. Reichman, R. Babbush, and J. Lee, *Nature* **603**, 416 (2022).
 - [20] T. E. O’Brien, M. Streif, N. C. Rubin, R. Santagati, Y. Su, W. J. Huggins, J. J. Goings, N. Moll, E. Klyseva, M. Degroote, *et al.*, *Physical Review Research* **4**, 043210 (2022).
 - [21] I. Avdic and D. A. Mazziotti, *Physical Review Letters* **132**, 220802 (2024).
 - [22] D. E. Koh and S. Grewal, *Quantum* **6**, 776 (2022).
 - [23] A. Zhao and A. Miyake, *npj Quantum Information* **10**, 57 (2024).

- [24] B. Wu and D. E. Koh, *npj Quantum Information* **10**, 39 (2024).
- [25] E. van den Berg, S. Bravyi, J. M. Gambetta, P. Jurcevic, D. Maslov, and K. Temme, *Phys. Rev. Res.* **5**, 033193 (2023).
- [26] J. Romero, R. Babbush, J. R. McClean, C. Hempel, P. J. Love, and A. Aspuru-Guzik, *Quantum Science and Technology* **4**, 014008 (2018).
- [27] R. J. Bartlett and M. Musiał, *Reviews of Modern Physics* **79**, 291 (2007).
- [28] I. G. Ryabinkin, T.-C. Yen, S. N. Genin, and A. F. Izmaylov, *Journal of Chemical Theory and Computation* **14**, 6317 (2018).
- [29] U. Aseguinolaza, N. Sobrino, G. Sobrino, J. Jornet-Somoza, and J. Borge, *Quantum Information Processing* **23** (2024), 10.1007/s11128-024-04384-z.

The submitted manuscript has been created by UChicago Argonne, LLC, Operator of Argonne National Laboratory (“Argonne”). Argonne, a U.S. Department of Energy Office of Science laboratory, is operated under Contract No. DE-AC02-06CH11357. The U.S. Government retains for itself, and others acting on its behalf, a paid-up nonexclusive, irrevocable worldwide license in said article to reproduce, prepare derivative works, distribute copies to the public, and perform publicly and display publicly, by or on behalf of the Government. The Department of Energy will provide public access to these results of federally sponsored research in accordance with the DOE Public Access Plan. <http://energy.gov/downloads/doe-public-access-plan>.